Carcinogenesis vol.33 no.6 pp.1158–1168, 2012
doi:10.1093/carcin/bgs138
Advance Access publication March 30, 2012

Folate deprivation enhances invasiveness of human colon cancer cells mediated by activation of sonic hedgehog signaling through promoter hypomethylation and cross action with transcription nuclear factor-kappa B pathway

Tz-Ping Wang[1], Shu-Han Hsu[1], Hsin-Chun Feng[1] and Rwei-Fen S.Huang[1,2,*]

[1]Department of Nutritional Science and [2]Ph.D. Program in Nutrition and Food Science, Fu Jen Catholic University, Xinzhuang, Taiwan, Republic of China

*To whom correspondence should be addressed. Department of Nutritional Science and Ph.D. Program in Nutrition and Food Science, Fu Jen Catholic University, Xinzhuang, Taiwan, Republic of China. Tel: +886 2 29052512; Fax: +886 2 29021215;
Email: 034825@mail.fju.edu.tw

Low folate status is well recognized as one of the metabolic stressors for colorectal cancer carcinogenesis, but its role in colon cancer invasion remains unknown. Activation of the Sonic hedgehog (Shh) signal in interaction with the transcription nuclear factor-kappa B (NF-κB) pathway is crucial for cancer aggressiveness. The aims of this study were to investigate whether and how folate deprivation promotes invasion by colon cancer cells in relation to Shh signaling and NF-κB pathway activation. Cultivation of epithelial colon carcinoma-derived cells (HCT116) in folate-deficient (FD) medium enhanced cellular migration and invasion, in correlation with epithelial–mesenchymal transition (EMT) associated with *Snail* expression and *E-cadherin* suppression, increased production of β1 integrin and increased proteolysis by matrix metalloproteinase 2. Blockade of Shh signaling by cyclopamine (CYC) or of NF-κB activation by BAY abolished FD-enhanced EMT and invasion by HCT116 cells. FD cells had 50–80% less intracellular folate, associated with aberrant hypomethylation of the *Shh* promoter, than control cells, and increased binding of nuclear NF-κB subunit p65 to the *Shh* promoter region, which coincided with increased *Shh* expression and protein production of Shh ligand; in addition, the FD-induced Shh signaling targeted *Gli1* transcription activator as well as *Ptch* receptor. The FD-induced Shh induction and activated signaling were blocked by NF-κB inhibitor BAY. Blockade of Shh signaling abrogated FD-promoted NF-κB activation measured by IκBα degradation and by target gene *TNFα* expression. Taken together, these findings demonstrate that folate deprivation enhanced invasiveness of colon cancer cells mediated by activation of Shh signaling through promoter hypomethylation and cross actions with the NF-κB pathway.

Introduction

Colorectal cancer (CRC) is one of the most lethal malignancies worldwide (1). Therapeutic options for CRC patients with metastatic cancers are limited, and the 5-year survival rate is <5% (2). Although the potential risk factors for CRC metastasis are not well understood, cancer cells acquire metastatic capacity via multistage epithelial–mesenchymal transition (EMT) (3). Alteration of EMT by increased *Snail* expression, which downregulates E-cadherin, an epithelial cell marker, could cause cancer cells to lose their epithelial junction and begin migration. Mesenchymal cancer cells express intermediate filaments and extracellular matrix components such as matrix metalloproteinase (MMP), enabling them to digest matrix protein for invasion. The adhesion molecule beta-integrin assists cancer cells in distant organ attachment (4). The induction of EMT via the activation of these molecular targets enhances the metastatic potential of cancer cells.

Recent advances show that aberrant activation of hedgehog (Hh) signaling contributes to EMT in the development of invasiveness and metastasis of several cancers (5–8). Hh signaling is activated when the mammalian Hh ligands such as Sonic hedgehog (Shh) or Indian hedgehog (Ihh) binds to its Patched (Ptch) receptor to release the repression of the activity of the transmembrane protein Smoothened (Smo) (9). Translocation of Smo into cytoplasm allows activation of the Gli transcription factors. *Gli1* is a target gene of Shh signaling, which messenger RNA (mRNA) expression is the reliable marker of pathway activity. Gli1 activates transcription of genes for Hh pathway components such as *Shh* ligand and *Ptch1* receptor (10) and EMT-associated targets (11,12). Overexpression of *Gli1* activator in mouse prostate carcinoma cells caused enhanced migration *in vitro* and lung metastasis *in vivo*, with induced *Snail* expression and *E-cadherin* repression (5). All the effects were inhibited by treatment with the pathway inhibitor cyclopamine (CYC). Studies have revealed that human colon epithelial cancer cells or human colon carcinomas displayed active Hh–Gli signaling, which is critical for tumor recurrence and metastasis (13,14). Chemical blockade of the Hh pathway by CYC inhibited colon cancer proliferation, tumor growth, EMT progress and metastasis (14,15).

Potential factors that promote the activation of Shh signaling in relation to colon cancer aggressiveness remain largely unknown. It has been proposed that the transcription nuclear factor-kappa B (NF-κB) plays a regulatory role in Hh signaling activation through Shh induction in cancers (16). The NF-κB pathway is the means of oncogenic signaling that orchestrates inflammatory responses, cellular proliferation, carcinogenesis and invasion by human cancer cells (17–20). In human colorectal tumor cells, NF-κB activation by lipopolysaccharide enhanced cellular adhesion and invasion through integrin 1-dependent mechanisms (21). NF-κB is composed of heterodimers or homodimers of the NF-κB/Rel family of proteins, whose activation is induced by several stimuli to release NF-κB complexes from inhibitory NF-κB (IκB) to translocate into the nucleus, whereas nuclear NF-κB subunit p65 may bind to a specific consensus sequence and regulate the transcription of target genes (22,23). When activated NF-κB p65 bound to the promoter region of the *Shh* gene, increased *Shh* expression and protein production promoted the growth of pancreatic cancers (17,24). Shh knockdown in an *in vivo* model of pancreatic cancer impaired NF-κB-mediated tumor growth (24). NF-κB-mediated activation of Shh signal in monocytes may contribute to pancreatic cancer progression through Shh production (25). In human renal cell carcinoma, the Shh signaling pathway is reactivated to interact with the NF-κB pathway, playing a critical role in tumor growth (26). Whether cross activation of Shh signaling with the NF-κB pathway contributes to colon cancer invasion requires investigation.

Colon cancer patients frequently suffer from folate deficiency due to dietary insufficiency, metabolic stress or clinical etiology such as inflammatory bowel diseases (27–30). Low folate status is well recognized as one of the metabolic stressors for CRC carcinogenesis (27–31). Cellular folate depletion disturbed intracellular one-carbon metabolism and thus the supply of methyl groups, leading to DNA hypomethylation and chromosome instability, in part explaining the carcinogenic action of folate deficiency in colon cancer (32). Whether folate insufficiency with disturbed one-carbon metabolism may predispose colon cancer cells to invasiveness is relatively unknown. Several key pathway elements of Hh signaling contain CpG islands in their promoter regions (33), and overexpression of *Shh* ligand by

Abbreviations: BAY, Bay117082; CRC, colorectal cancer; CYC, cyclopamine; EMSA, electrophoretic mobility shift assay; EMT, epithelial-mesenchymal transition; FBS, fetal bovine serum; FD, folate-deficient; Hh, Hedgehog; Ihh, indian hedgehog; LY, LY294002; MMP, matrix metalloproteinase; mRNA, messenger RNA; MTX, methotrexate; NF-κB, nuclear factor-kappa B; PI, propidium iodide; Ptch, patched; Shh, sonic hedgehog; Smo, smoothened.

epigenetic demethylation of its promoter region has recently been reported in primary colorectal carcinoma (34). Promoter hypomethylation is suggested to be an important mechanism regulating constitutive *Shh* expression in cancer aggressiveness (35). In addition, prolonged folate deprivation induced the expression of invasive-associated genes such as those for NF-κB and for the adhesion molecule integrin 1 in human colon adenocarcinoma cell lines (36). The limited evidence raises the possibility that folate deficiency promotes colon cancer invasiveness through the activation of these two invasive-associated signaling routes.

The aims of this study were to investigate whether and how folate deprivation promotes invasion by colon cancer cells in association with Shh signaling and the NF-κB pathway. We used the HCT116 cell line, which has low invasive capacity, as an *in vitro* cell model, as it derives from an adenocarcinoma of the colorectal epithelium with adenomatous polyposis coli (*APC*) tumor suppressor gene mutations and thus mimics an aberrant molecular background in colon cancer lesions. We report, for the first time, that folate deprivation enhanced invasion by colon cancer cells mediated by activation of Shh signaling through *Shh* promoter hypomethylation and cross actions with NF-κB pathways.

Materials and methods

Materials

Folate (pteroylmonoglutamic acid), methotrexate (MTX), CYC, and McCoy's 5A medium were purchased from Sigma Chemical (St Louis, MO). RPMI 1640 medium was obtained from Invitrogen (Grand Island, NY). Penicillin, streptomycin, fungizone, trypsin, trypan blue and fetal bovine serum (FBS) came from Gibco Laboratories (Grand Island, NY). Matrigel was purchased from BD (Franklin Lakes, NJ). NF-κB inhibitor Bay117082 (BAY), PI3K inhibitor LY294002 (LY) and antibodies of NF-κB, IκBα, pIκBα (Ser^{32}), Shh, Gli1, integrin β1, MMP2 and 9 were from Cell Signaling Technology (Boston, MA). Antibodies for β-actin and histone H1 were from Millipore (Temecula, CA) and GeneTex (Irvine, CA), respectively. Millicell culture inserts containing a thin-film polycarbonate (PCF) membrane with a pore size of 8 μm were obtained from Millipore (Billerica, MA).

Cell culture

The HCT116 cell line was obtained from the National Development Center of Biotechnology (Taipei, Taiwan). HCT116 cells were maintained as a monolayer culture in McCoy's 5A medium at 37°C in a humidified 5% CO_2 incubator with the medium changed every 3 days. Before the experimental treatment, the cells were adapted to culture in RPMI 1640 medium supplemented with 2.0 g/l sodium bicarbonate, 10% (vol/vol) FBS, 100 U/ml of penicillin and 100 mg/ml of streptomycin. Folate-deprived cells were cultured in folate-deficient (FD) RPMI 1640 medium to deplete intracellular folate levels. To minimize exogenous folate sources, we replaced FBS with dialyzed FBS, which had been dialyzed against phosphate-buffered saline at 4°C for 16 h. As the folic acid antagonist, MTX treatment (100 μg/ml) was used to disrupt intracellular one-carbon metabolism, serving as the alternative folate-deprived control in some of the experiments.

Migration and invasion assays

Migration of HCT116 cells was examined by modified Millicell culture insert. After the inner side of the PCF membrane was precoated with 100 μl matrigel (2 mg/ml) overnight, we measured cellular invasiveness. Cellular migration was measured using the insert without matrigel coating. A cell suspension (5×10^4 cells) was added to each insert. The cells were allowed to migrate or invade for 24 or 48 h at 37°C and 5% CO_2. The cells that invaded or migrated through the pores and adhered to the PCF membrane were fixed and dipped in methyl alcohol for 15 min. The PCF membranes were dyed for 1 h with Giemsa stain and then the invaded cells were observed and recorded under the microscope. The results were expressed as number of invaded cells per microscope field. All experiments were repeated three to six times.

Cancer cell adhesion

HCT116 cell attachment to collagen I was performed as described previously with some modifications (21). Briefly, collagen I (1.5 μg/ml) was coated onto 96-well plates and incubated for 15 h at 4°C. HCT116 cells cultivated in various experimental media at different time periods were passed into the collagen I-coated 96-well plates and incubated in serum-free medium at 37°C in humidified 5% CO_2 for 2 h. The plates were washed twice with phosphate-buffered saline to remove unbound cells. Then the absorbance was decided by the MTT colorimetric method.

Gelatin zymography

The activities of MMP-2 and MMP-9 in the conditioned media (serum free) were determined by gelatin zymography. One hour before cultivation of HCT116 cells was terminated at each designated time point, the medium changed to conditioned medium. The conditioned media were collected and centrifuged. The supernatants were then loaded onto sodium dodecyl sulfate–polyacrylamide gels that were polymerized with gelatin at a final concentration of 0.1 mg/ml. After electrophoresis, the gels were renatured in 2.5% Triton X-100 and then incubated in developing buffer (40 mM Tris–HCl buffer, pH 7.4) in the presence of 2 mM $CaCl_2$ and 0.01% NaN_3 overnight at 37°C. The gels were then stained with Fast Blue gel staining reagent (Protech, Taipei, Taiwan). The gelatinase activity of MMP2 or MMP9 was then visualized as transparent bands on a blue background.

RNA extraction and real-time reverse transcription–PCR

Total RNA was extracted with an RNAzol Bee-RNA isolation kit. Briefly, 1 μg of each sample was reverse-transcribed in an MMLV Reverse Transcriptase 1st-Strand cDNA Synthesis Kit. Gene transcripts were amplified with specific primers as shown in the Supplementary Table 1, available at *Carcinogenesis* Online. The cycling conditions included an initial phase of 2 min at 50°C, 10 min at 95°C and then 40 cycles of 10 s at 95°C, 0.5 min at 60°C and 10 s at 72°C. Amplified complementary DNA was quantified using the QuantiTect SYBR Green PCR kit in a LightCycler PCR system.

Western blotting

Whole-cell extraction was conducted using cell lysis buffer (Cell Signaling Technology, Boston, MA) supplemented with 10 mM protease inhibitor cocktail and 1 mM phenylmethylsulfonyl fluoride. Protein concentrations were then measured with Bio-Rad protein assay kits (Bio-Rad, Hercules, CA). The protein lysates were resolved by sodium dodecyl sulfate–polyacrylamide gel electrophoresis and then transferred onto polyvinylidene difluoride membranes (Whatman, Boston, MA), blocked with phosphate-buffered saline containing 0.2% Tween 20 and 5% non-fat powdered milk and incubated first with antibodies. Bound antibodies were detected using Anti-mouse or anti-rabbit secondary antibody horseradish peroxidase conjugate (Santa Cruz Biotechnology, Santa Cruz, CA), followed by SuperSignal West Femto Chemiluminescent Substrate (Thermo, Rockford, IL) using a UVP BioSpectrum system (Upland, CA).

Electrophoretic mobility shift assay

Nuclear proteins were prepared with a Nuclear Extraction Kit (Panomics, Fremont, CA). Oligonucleotides (sense strand: 5′-AGTTGAGGGGACTCTCCCAGGC-3′; antisense strand: 5′-GCCTGGGAGAGTCCCCTCAACT-3′) corresponding to the binding sequences for NF-κB in the *Shh* promoter were biotin labeled (24). Electrophoretic mobility shift assay (EMSA) was performed using an EMSA "Gel Shift" Kit (Panomics, Fremont, CA). One microgram of NF-κB subunit p65 rabbit polyclonal antibodies (Chemicon, Temecula, CA) was added to the binding reactions and incubated for 1 h at room temperature before the addition of labeled oligonucleotides. The specificity of the assay was determined by including a 100-fold excess of unlabeled oligonucleotide in the binding mixture. After electrophoresis, gels were dried, the biotin end-labeled DNA was detected using streptavidin–horseradish peroxidase conjugate, and the signals were then detected using the UVP BioSpectrum system.

Enzyme-linked immunosorbent assay of NF-κB activation DNA binding

The TransAM™ NFκB p65 kit (Active Motif, Tokyo, Japan) was used according to the manufacturer's instructions. A double-stranded DNA sequence containing the NF-κB binding consensus site (5′-GGGACTTTCC-3′) was immobilized to the 96-well plate. Nuclear extracts of the HCT116 cells cultivated in each condition were applied to the wells and allowed to bind to the response element. NF-κB DNA binding was detected by the subsequent addition of a primary antibody against p65 and a horseradish peroxidase-conjugated secondary antibody. A colorimetric readout was obtained at 450 nm using a Bio-Rad plate reader.

Analysis of apoptotic and necrotic cells

Cells (1×10^6) were suspended in incubation buffer (10 mmol/l *N*-2-hydroxyethylpiperazine-*N*′-2-ethanesulfonic acid /NaOH, pH 7.4, 140 mmol/l NaCl and 5 mmol/l $CaCl_2$) containing 1 mg/l propidium iodide (PI) and a 1:50 dilution of Annexin-V-Fluos labeling solution. The mixed solution was incubated for 15 min on ice. Incubation buffer was added, and green (annexin-V stain: apoptotic cells) and red (PI stain: necrotic cells) fluorescence intensities were analyzed on a Coulter EPICS XL-MCL flow cytometer (Coulter, Miami, FL) at 488 nm excitation with a 515 nm bandpass filter for annexin V and a 560 nm filter for PI detection. Cells positive for Annexin-V and negative for PI fluorescence were defined as apoptotic.

Intracellular folate assay

Intracellular folate levels were determined by the method of Horne and Patterson (37). Briefly, cells from control or FD cultures were trypsinized, and intracellular folate was extracted in extraction buffer [20 g/l sodium ascorbate, 50 mmol/l *N*-2-hydroxyethylpiperazine-*N*′-2-ethanesulfonic acid, 50 mmol/l CHES (2-[*N*-cyclohexylamino]-ethanesulfonic acid), 1.4% β-mercaptoethanol, pH 7.85]. Upon treatment with chicken pancreas conjugase (vol/vol: 4:1), total intracellular folate content was quantified by microbiological assay using glycerol-protected *Lactobacillus casei* (ATCC no. 7469) in 96-well microtiter plates. Absorbance was measured at 600 nm in an MRX model ELISA reader (Dynatech Laboratories, West Sussex, UK).

Bisulfite modification of genomic DNA

Genomic DNA was isolated using the standard protocol. Bisulfite modification of genomic DNA was performed in an EpiTect PCR Control DNA Set (Qiagen, Hilden, Germany). This procedure integrates DNA denaturation and bisulfite conversion into one step based on a reaction between cytosine and sodium bisulfite that converts unmethylated cytosines into uracils. Briefly, 1 μg DNA in 20 μl de-ionized water was mixed with CT Conversion Reagent and heated at 95°C for 10 min and then at 64°C for 2.5 h. Binding buffer was added, and the sample was applied to a Zymo-Spin^{TM} IC column for centrifuging at full speed (≥10 000*g*) for 30 s. The supernatant was incubated in desulfonation buffer for 20 min. Each bisulfited DNA sample was eluted from the column matrix in 10 μl Tris-EDTA buffer and stored at or below –20°C.

Analysis of CpG island methylation status of Shh promoter

The *Shh* promoter exists as a dense CpG island spanning ∼300 bp around the first exon (38). DNA methylation patterns of the CpG islands of the *Shh* promoter were determined by bisulfite modification of the unmethylated, but not the methylated, cytosines to uracil and subsequent PCR using primers specific to either the methylated or the modified unmethylated DNA. The primers were designed as either 'M' primers to detect methylated DNA sequences (forward: 5′-GGAGAGTTTTTCGTAGTCGC-3′; reverse : 5′-CGTATACGCTCT CTCTTACGC-3′) or 'U' primers to detect nmethylated sequences (forward: 5′-GGTGGAGAGTTTTTTGTAGTTGT-3′; reverse: 5′-ACATATACACTCTCTCTTACACTT-3′). The products of this methylation-specific PCR were 131 bp long for unmethylated DNA and 127 bp long for methylated DNA. The conditions for the methylation-specific PCR were an initial denaturation at 95°C for 10 min; 40 cycles of 94°C for 30 s, 54°C for 45 s, 72°C for 45 s and a final extension at 72°C for 10 min. Human placental DNA treated *in vitro* with *Sss*I methyltransferase was used as a positive control for methylated alleles and DNA from normal lymphocytes as a negative control for methylated alleles. Each PCR reaction was directly loaded into 2% agarose gels, stained with ethidium bromide and visualized under UV illumination.

Statistics

Data were analyzed by Student's paired *t*-test to determine the statistical significance of differences between the control and folate-deficient groups at $P = 0.05$.

Results

Folate deprivation and MTX treatment enhanced invasiveness of HCT116 cells

HCT116 cells cultured in FD medium for 24 and 48 h showed greater migration and invasion than control cells (Figure 1A). Migration was increased to 2× after 24 h and to 7× after 48 h ($P < 0.05$; Figure 1B). Invasion of matrigel was increased to 2× and 5×, respectively ($P < 0.05$; Figure 1B). Adhesion was significantly increased too (Figure 1C). As cell viability may compromise the invasive and adhesive phenotype of cancer cells, we further characterized apoptotic and necrotic cellular death (Supplementary Figure 1 is available at *Carcinogenesis* Online). FD treatment for 24 and 48 h induced apoptosis of up to 10% of cells (AV-positive), compared with 5% of the controls ($P < 0.05$), without affecting overall necrosis (PI-positive; <5%). To confirm that the enhanced invasion by FD cells was specific to the disturbance of intracellular one-carbon metabolism due to folate depletion, we used MTX, a folate antimetabolite, as the alternative FD control. Treatment of HCT116 cells with MTX for 24 h significantly induced migration, invasion and adhesion (Figure 1A–C). Relative to the controls, FD cultivation of HCT116 cells induced proteolysis by MMP-2 in the pro-form and the active form at 6, 12 and 24 h ($P < 0.05$; Figure 1D). Activities of MMP-9 showed no response to FD (data not shown). The production of β1 integrin was increased at 12–24 h ($P < 0.05$; Figure 1E). MTX treatment significantly increased the activities of pro- and processed-MMP-2 and increased the production of β1 integrin (Figure 1D and E). It also promoted apoptosis of 20% and necrosis of 7% (Supplementary Figure 1 is available at *Carcinogenesis* Online).

Inhibition of Hh signaling and NF-κB pathway abolished FD-induced EMT and invasion by HCT116 cells

Both Hh signaling and the NF-κB pathway are crucial for colon cancer invasion. We investigated their involvement in FD-enhanced invasion by HCT116 cells. Pretreatment of FD cells with CYC to inactivate Hh signaling or with BAY to inhibit NF-κB activation completely abrogated FD-enhanced invasion by HCT116 cells (Figure 2A and B). CYC or BAY treatment did not significantly affect cellular viability during the experiment (data not shown). FD increased expression of *Snail* and suppressed expression of *E-cadherin* (Figure 2C and D). CYC or BAY treatment of FD cells abolished FD-enhanced EMT markers and proteolytic MMP-2 activity (Figure 2C–E). The data thus suggest that FD-enhanced EMT and invasion by HCT116 cells was in part, if not all, mediated by activation of Hh signaling and the NF-κB pathway.

Depleted intracellular folate status was associated with aberrant methylation status of the Shh promoter region in FD cells

To investigate how folate depletion may activate Shh signaling, we analyzed both the intracellular folate level and the methylation status of the *Shh* promoter region. Intracellular folate levels of FD cells dropped significantly by 50% at 6 h, by 60% at 12 h and by 80% at 24 and 48 h ($P < 0.05$; Figure 3A). As the *Shh* promoter harbors a dense CpG island spanning ∼300 bp around the first exon (38), we analyzed methylation of the promoter region by the bisulfite method and methylation-specific PCR analysis (Figure 3B). In the control cells, the *Shh* promoter region was partially methylated during 6, 12 and 24 h cultivation. In the FD cells, the methylation status gradually decreased at 12 and 24 h, as shown by the reduced amplification by the M primer (Figure 3B). Hypomethylation of the *Shh* promoter was complete at 24 h.

Effects of FD on Shh induction and Shh–Gli signaling

To delineate the FD-associated hypomethylation from Shh induction and Hh signaling, we assayed transcript and protein levels of Shh, the key pathway components and target genes of Hh signaling (Figure 4). Transcript levels of *Shh* were significantly increased to 2.0–2.5× at 6, 12 and 24 h ($P < 0.05$; Figure 4A). The production of Shh ligand was significantly raised to 2× at 12 and 24 h ($P < 0.05$; Figure 4B). Simultaneously, transcripts and proteins of transcription factor Gli1, one of the targets of activated Hh signaling, were upregulated to 2–3× at 6–24 h (Figure 4B). To further confirm FD-activated Hh signaling, we assayed expression of another target gene, Ptch receptor, and other pathway components, namely Ihh ligand, Smo transducer and Hip repressor. Except for *Hip*, all target genes and pathway components were upregulated in FD cells (Figure 4C). MTX treatment promoted activation of the Shh–Gli signal via increased production of Shh ligand and effector Gli1 (Figure 4B).

Effects of FD on NF-κB activation associated with increased DNA binding to Shh promoter region

We further investigated whether and how FD-induced Shh signal related to NF-κB activation. Production of the RelA/p65 subunit of NF-κB was first upregulated at 6 h of FD cultivation and remained increased levels at 12 and 24 h ($P < 0.05$; Figure 5A). Treatment of HCT116 cells with MTX also increased RelA/p65 ($P < 0.05$). To directly assess the effects of FD-increased RelA/p65 on Shh induction, we used an oligonucleotide corresponding to putative NF-κB binding sites within the *Shh* promoter region (17,24) to perform EMSA. Relative to the control nuclear extract, 6 h FD cultivation enhanced DNA binding of nuclear NF-κB to the *Shh* promoter region, as indicated by the increased intensity of the shifted band of the protein–DNA

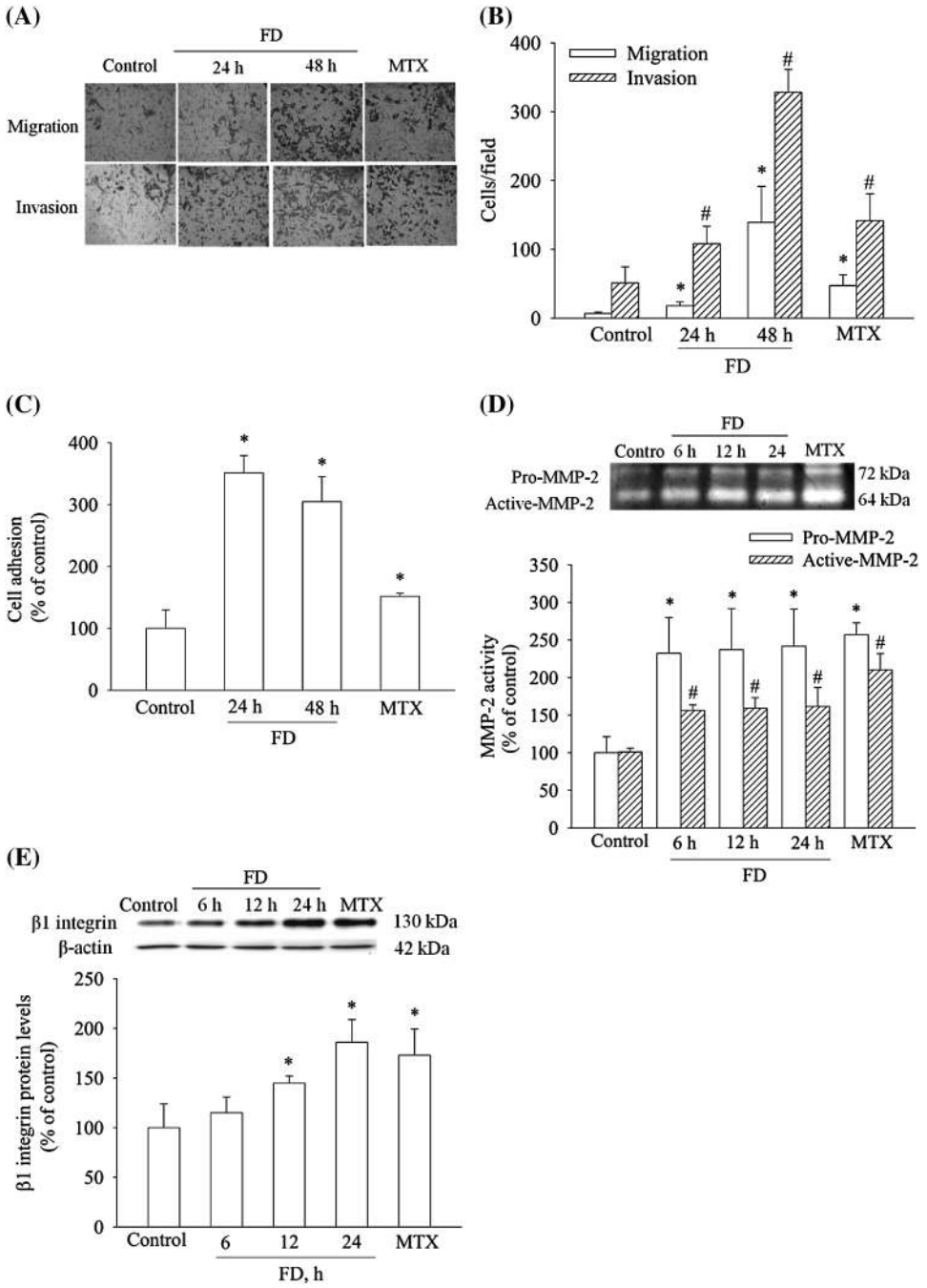

Fig. 1. Effects of folate deprivation on invasiveness of HCT116 cells. HCT116 cells at log-growth phase were cultured with control or folate deficient (FD) medium for 6, 12, 24 or 48 h or with control + MTX (100 μg/ml) medium for 24 h. (**A**) Representative matrigel images of migration and invasion by HCT116 cells. (**B**) Quantification of invasive or migration cells by counting Coomassie blue-stained cells in 10 fields of each multicell PCF insert. (**C**) Cancer cell adhesion. (**D**) Proteolytic activities of MMP-2 and (**E**) Production of β1 integrin adhesion molecules. The proteolytic activities of MMP-2 were measured by gelatin zymographic assay. β1 Integrin production was assayed by western blot. Data are means ± standard deviations of three to six independent experiments or the percentages of control (means ± standard deviations of three independent experiments). *, #Compared with respective controls by Student's *t*-test at $P < 0.05$.

complex (Figure 5B, left panel). Correspondingly, immunoblots for RelA performed on nuclear extracts confirmed that the NF-κB protein–DNA complex contained p65 (Figure 5B, super-shift). The shifted band specific to NF-κB binding was identified by competition with unlabeled NF-κB at 100× concentration (cold competition). The unlabeled oligonucleotide effectively competes with binding, leading to the disappearance of the band on the nuclear extracts of the control and FD cells at 24 h (Figure 5C). The competition assay confirmed that the nuclear protein subunits binding to the Shh promoter are specific for the NF-κB consensus binding sequence.

Blockade of NF-κB pathway abolished FD-induced Shh induction and Shh–Gli signaling by HCT116 cells

We further investigated whether FD-promoted Shh induction and Shh–Gli signaling depended on NF-κB pathway activation. Pretreatment of HCT116 cells with BAY abrogated FD-promoted transcript and protein levels of the Shh ligand during 6 to 24 h cultivation (Figure 6A and C; some data not shown), which in parallel diminished the response of the FD-induced target gene *Gli1* (Figure 6B and C) in Shh signaling. The data suggest that NF-κB pathway activation mediated Shh signaling partially, if not totally, through Shh ligand

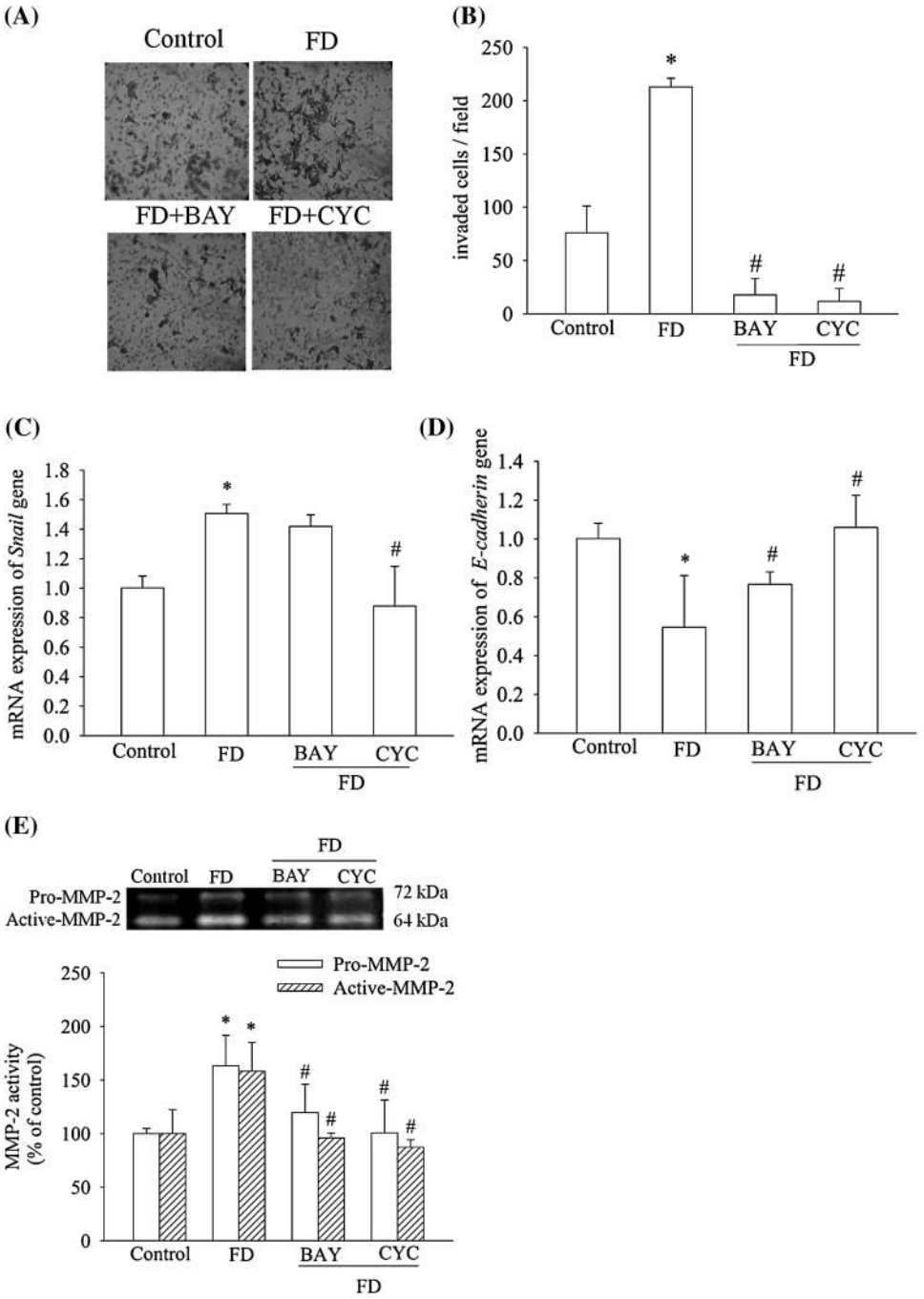

Fig. 2. Effects of Hh and NF-κB pathway inhibitor treatment on FD-induced EMT and invasion by HCT116 cells. HCT116 cells at log-growth phase were cultivated in control or folate deficient (FD) medium for 24 h with or without 24 h pretreatment with cyclopamine (CYC: 10 μM) or Bay117082 (BAY: 3 μM). Expression of EMT molecular markers and invasion by HCT116 cells were assayed. (**A**) Representative matrigel images of invasion by HCT116 cells. (**B**) Quantification of invasive cells by counting Coomassie blue-stained cells in 10 fields of each multicell PCF insert. (**C** and **D**) Transcript expression of EMT markers (C) *Snail* and (D) *E-cadherin* was assayed by reverse transcription–PCR. The PCR products were corrected for the corresponding level of *GUS* gene in each sample. (**E**) The proteolytic activities of MMP-2 were measured by gelatin zymographic assay. Data are the percentages of the control. Values are mean ± standard deviation of three independent experiments. *Compared with the respective control; #compared with the respective FD group by Student's t-test at $P < 0.05$.

induction in FD cells. To confirm whether the NF-κB-mediated Shh signaling was Shh induction dependent, we tested with CYC as a potent inhibitor of Smo, a Shh-dependent signal transducer. Treatment of FD cells with CYC completely abolished FD promotion of transcript and protein levels of Shh and Hh target genes of *Gli1* (Figure 6A–C). It should be noted that CYC treatment of 12 h FD cells significantly reduced the *Gli1* transcript levels to below the controls, suggesting that Shh–Gli signaling accounts for the residual Hh activation in the control cells. When FD cultivation reached 24 h, the *Gli1* transcript levels of the CYC-treated FD cells had rebounded to the control levels (Figure 6B).

Blockade of Shh signaling differentially affected FD-induced NF-κB pathway activation of HCT116 cells

The next question to ask was whether FD-induced Shh signaling cross-reacted with NF-κB pathway, as previously reported in several cancer cells (26). At transcriptional levels, FD promoted mRNA expression of NF-κB subunit p65 only at 6 h cultivation. BAY or

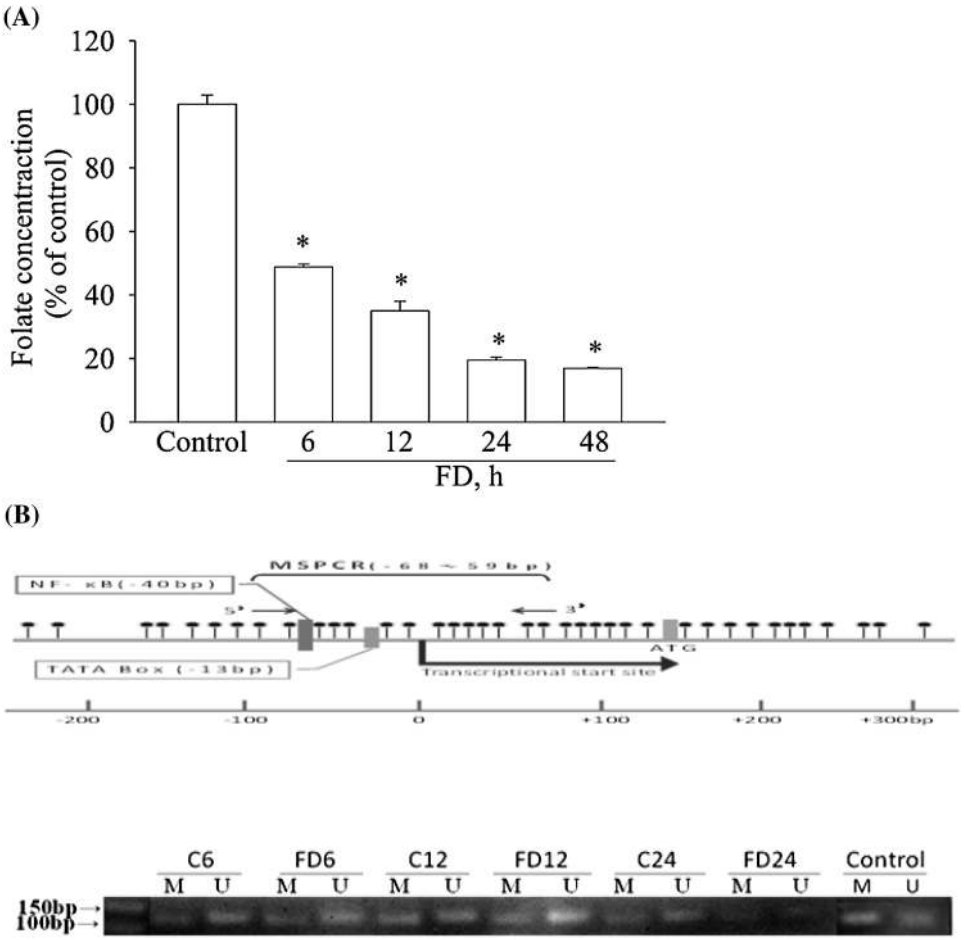

Fig. 3. Effects of folate deprivation on intracellular folate status and methylation status of the *Shh* promoter region in HCT116 cells. HCT116 cells at log-growth phase were cultivated in control (C) or folate deficient (FD) medium for 6, 12, 24 or 48 h. (**A**) Intracellular folate levels of HCT116 cells. Data are percentages of the control. Values are means ± standard deviations of three independent experiments. *Compared with the control by Student's *t*-test at $P < 0.05$.
(**B**) Representative graph showing the region between –200 and +300 of the *Shh* 5′-flanking sites. The locations of the primers for methylation-specific (MS) PCR lay in the –68 to –59 bp region. Analysis of CpG island promoter methylation status of the *Shh* gene by MSP in DNAs of cells cultivated for 6–24 h. The presence of a visible PCR product in lane M indicates the methylated promoter region, and the presence of product in lane U indicates the unmethylated promoter region. Normal human DNA (Control U) and *in vitro* methylated DNA (Control M) were used as negative and positive controls for methylation, respectively.

CYC treatment did not affect FD-induced *RelA/p65* transcript levels (Supplementary Figure 2 is available at *Carcinogenesis* Online). Blockade of RelA/p65 activation by BAY abolished FD-induced levels of the RelA/p65 subunit (Figure 7A). Treatment of FD cells with CYC completely abolished it (Figure 7A). Using *TNFα* as one of the target genes of activated NF-κB signaling as a marker, we found that both BAY and CYC treatment abolished FD-induced expression of *TNFα* (Figure 7B), suggesting that the FD-activated Shh–Gli signal may interact with the NF-κB signaling in HCT116 cells.

FD significantly promoted IκBα degradation in the cytosolic extract, as evidenced by decreased IκBα levels at 12 and 24 h cultivation ($P < 0.05$; Figure 7C). Treatment of HCT116 cells with CYC abolished FD-induced IκBα degradation. Treatment of cells with LY, a PI3K/Akt inhibitor, abrogated FD-induced IκBα degradation (Figure 7C), suggesting that FD-induced NF-κB activation is involved in the PI3K/Akt signal. pIκBα (Ser^{32}) was barely detected in the sample extracts, probably owing to the rapid turnover of this subunit form (data not shown). As shown by altered levels of NF-κB subunit p65 in nuclear extract, FD-promoted nuclear translocation of the NF-κB p65 subunit was most evident at 12 h and was decreased at 24 h, when treatment with inhibitors, including CYC, had no effect (Figure 7C). Similarly, FD increased the peak of nuclear NF-κB DNA binding activity at 12 h (Figure 7D), following which the activity was reduced. CYC treatment did not modulate nuclear NF-κB DNA-binding activity at 24 h. The data suggest that the FD-induced Shh signal differentially affected the FD-promoted NF-κB pathway activation of HCT116 cells. Both BAY and LY increased NF-κB DNA-binding activity of 24 h FD cells, again suggesting the existence of a yet-unidentified FD-associated suppressive mechanism by which PI3K/Akt or NF-κB activation may negatively affect its DNA binding activity.

Discussion

Because low folate status is well established as a risk factor for CRC carcinogenesis (27–31), we tested the hypothesis that it may lead colon cancer cells to develop aggressiveness. Several lines of evidence indicate that folate deprivation enhanced the invasiveness of HCT116 cells: (i) FD induced upregulated *Snail* expression and suppressed *E-cadherin* expression, causing loss of epithelial adhesion and thus promoting migration (39). (ii) FD increased the proteolytic activity of MMP-2, which digested Type I collagen in extracellular matrix, permitting invasion (3). (iii) FD-promoted mRNA expression (36) and protein production of β1 integrin (a fibronectin receptor), which supports the attachment of cancer cells to extracellular matrix (40). The FD-induced alteration of EMT molecular markers correlated with low intracellular folate status of colon cancer cells (80% depletion). Previous evidence suggests that low-folate-induced aberrant one-carbon metabolism in colon cancers (27–32) is responsible. Indeed, treatment of HCT116 cells with a folate antimetabolite, MTX, promoted

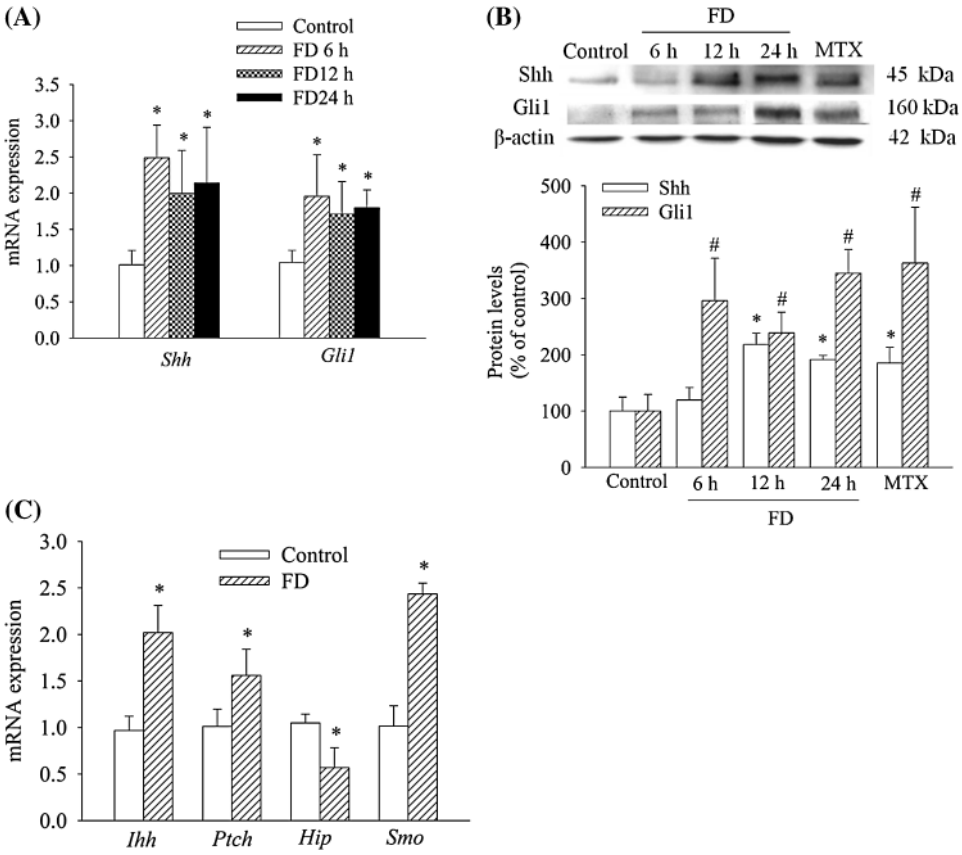

Fig. 4. Folate deprivation activated Shh induction and Hh signaling. HCT116 cells were cultivated in control, folate deficient (FD) or control + MTX medium (100 μg/ml) for 6, 12 or 24 h. (**A**) Transcript levels of Shh ligand and Gli1 transcription activator in control or FD HCT116 cells. (**B**) Production of Shh ligand and Gli activator proteins. 'MTX' indicates cells cultivated in control medium + MTX (100 μg/ml) for 24 h. (**C**) Transcript levels of pathway components and target genes of Shh signaling as assayed by RT–PCR. Changes in the specific PCR products were corrected for the corresponding level of *GUS* gene in the sample. Protein production was analyzed by western blot. Data are percentages of the control. Values are means ± standard deviations of three independent experiments. *, #Compared with the respective controls by Student's *t*-test at $P < 0.05$.

proteolytic MMP-2 activities, induced expression of β1 integrin and enhanced migration and invasiveness of HCT116 cells. Taken together, our data identify folate deprivation as a one-carbon metabolic stressor that promotes EMT and enhances the invasiveness of colon cancer cells.

Aberrant activation of Hh signaling by dysregulation of Hh ligands such as Shh or downstream components of the Hh–Gli pathway has been shown to be associated with the aggressiveness of cancers (5–8), including colon cancers (13–15). Consistent with these scenarios, we demonstrated that FD promoted aberrant activation of Shh–Gli signaling, which modulated the invasiveness of HCT116 cells. Several studies have reported that HCT116 cells possessed a low residual Hh signal characterized by the absence of *Patch* mRNA, the absence of Shh ligand (41), low Hh reporter activity (42) and no response to CYC, which inhibited Shh signaling by binding to Smo (43). With upregulating Shh, FD activated Hh signaling, as evidenced by increased mRNA expression of transcription activator *Gli1* and receptor *Patch*, target genes of the Hh signal pathway (9,10). As *Snail* induction and *E-cadherin* suppression (markers of EMT) were early responses to *Gli1* overexpression (11), blockade of Hh signaling by CYC downregulated FD-induced *Shh* and *Gli1* expression and completely abolished FD-enhanced EMT and invasion by colon cancer cells. These concordant results indicate that FD aberrantly activated Shh induction and Shh–Gli signaling, enhancing EMT and invasion by HCT116 cells.

The precise nature of FD-induced Shh overproduction and activated Shh signaling in colon cancer cells remains elusive. One plausible mechanism is persistent induction of Shh ligand through hypomethylation of its gene's promoter region (35). Overproduction of Shh and hypomethylation within the promoter correlated with increased gene expression in primary CRCs (34) and in microsatellite and chromosomal stable colon cancers (44). Consistent with a low residual Hh signal in some colon cancer cell lines (41–43), absence of *Shh* mRNA expression and hypermethylation of its promoter were reported (34). In agreement with the previous studies, we found partial methylation of the *Shh* promoter region and low residual expression of transcripts and proteins in HCT116 cells. FD depleted the intracellular folate content of HCT116 cells by 50–80%, and this depletion correlated with hypomethylation of the CpG region of the *Shh* promoter and correspondingly with elevated expression of Shh transcripts and protein. *Ihh* with a hypermethylated promoter region was not expressed in colon cancer cell lines (34) but was upregulated in FD HCT116 cells. Our preliminary data showed that blockade of transmethylation by 5-aza-2′-deoxycytidine increased *Shh* and *Ihh* expression in colon adenocarcinoma cells, and 5-aza-2′-deoxycytidine treatment of FD colon cancer cells further promoted *Shh* and *Ihh* expression (45). *Shh* expression and Shh signaling were also induced in MTX-treated HCT116 cells. Taken together, our data confirm the canonical impact of folate deprivation as a one-carbon metabolic stressor that influences aberrant promoter region-specific hypomethylation of Shh pathway components. This role of folate deprivation in hypomethylation of the *Shh* promoter may contribute in part, if not all, to the activated Hh pathway in FD-enhanced colon cancer invasion.

Alternatively, FD promoted the NF-κB activation to contribute to Shh signaling through Shh ligand induction. Enhanced binding of nuclear NF-κB p65 to the *Shh* promoter with increased transcript levels of *Shh* was shown in 6 h FD cells, followed by increased Shh protein production at 12 h. Blockage of NF-κB activation by BAY abolished FD-induced transcript levels of *Shh* and *Gli1*, a target gene

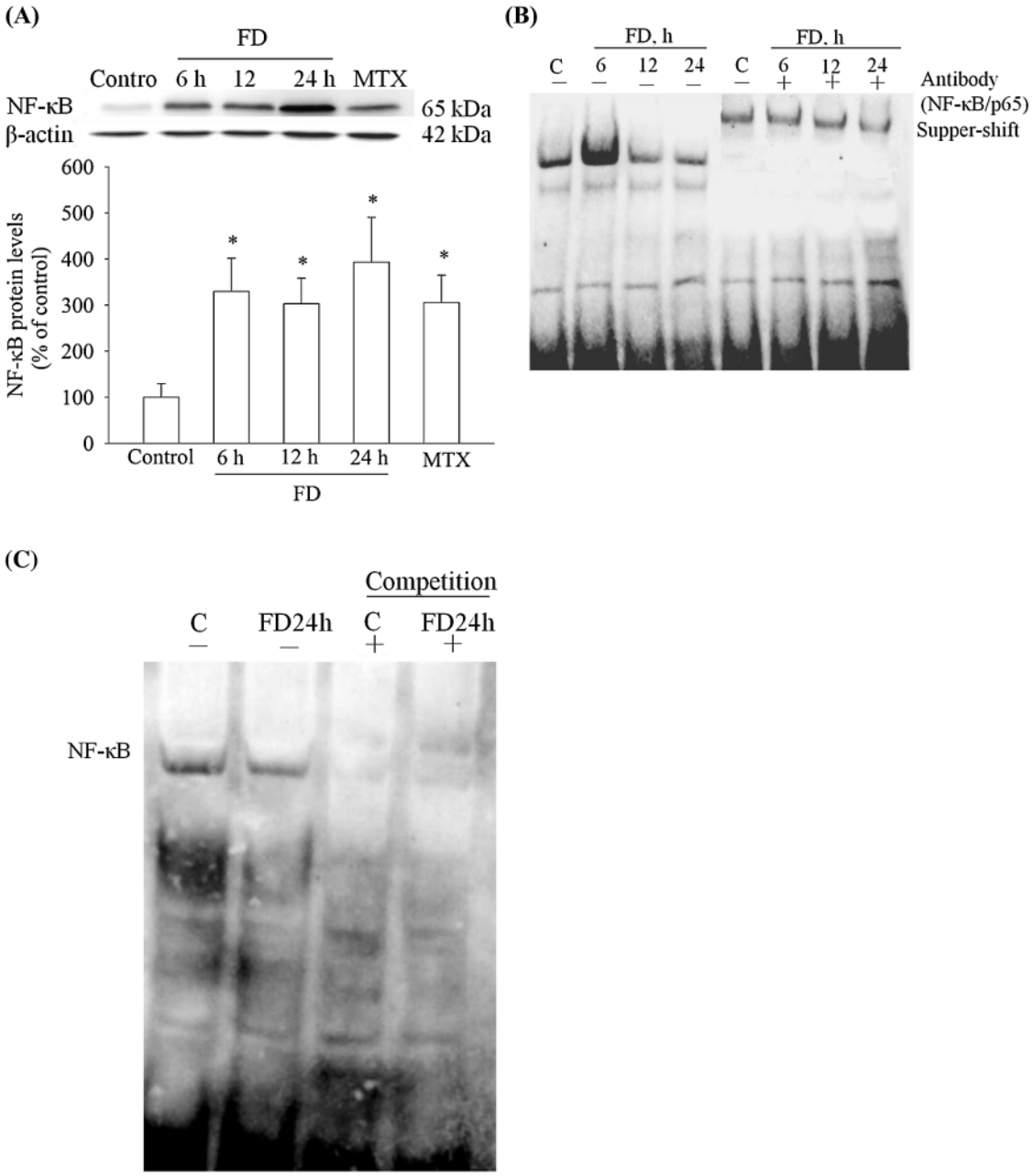

Fig. 5. Effects of folate deprivation on NF-κB activation in DNA-binding activity of the *Shh* promoter region. HCT116 cells were cultivated in control, folate deficient (FD) or control + MTX medium (100 μg/ml) for 6, 12 or 24 h. (**A**) Production of total NF-κB p65 subunit was analyzed by western blot. (**B**) The nuclear NF-κB subunit p65 binding activity of the *Shh* promoter region measured by EMSA and immunoblot. Electrophoresis gel shows bands of biotin-labeled NF-κB-binding oligonucleotide in the *Shh* promoter shifted by binding to nuclear protein extracts from the control and FD cells, indicating formation of DNA–protein complexes. Immunoblots for NF-κB/p65 are identified as super-shift bands. (**C**) The competition assay showed that the nuclear protein subunits binding to the Shh promoter are specific for the NF-κB consensus binding sequence. The shifted band specific to NF-κB binding was identified by competition with unlabeled NF-κB oligonucleotide at 100× concentration. In nuclear proteins extracted from 24 h cultivated control and FD cells, unlabeled NF-κB oligonucleotide competes with binding (cold competition). Results are representative of two separate experiments.

of Shh signaling. The data suggest that Shh ligand is the downstream target of the FD-promoted NF-κB pathway at the transcriptional level in colon cancer cells. Such actions of the NF-κB activation on the Shh signaling pathway, newly identified in FD-colon cancer cells, are in agreement with recent findings that overproduction of NF-κB p65 increased nuclear p65 binding to the *Shh* promoter *in vivo*, increasing *Shh* expression and so mediating pancreatic tumorigenesis and aggressiveness (17,24,25). Interestingly, we found that FD-enhanced NF-κB p65 binding to the *Shh* promoter region was decreased after 6 h cultivation, whereas NF-κB activity was persistently upregulated by FD-enhanced IκB protein degradation, increased protein levels and its target gene expression of *TNFα* (Figure 7). This FD-promoted NF-κB activation was consistent with the results of our previous report on human hepatoma cells (46). A substantial variety of mechanisms regulate the DNA-binding activity of various NF-κB homo- and hetero-dimers. The strength and duration of the NF-κB binding to the promoters of target genes may in part, or in total, rely on posttranslational modifications such as acetylation or phosphorylation of the NF-κB complex or relevant histones around NF-κB target genes (47,48). Given that total DNA-binding activity of NF-κB was also decreased after 12 h FD cultivation (Figure 7), when the *Shh* promoter region started to be hypomethylated by folate deprivation (Figure 3)

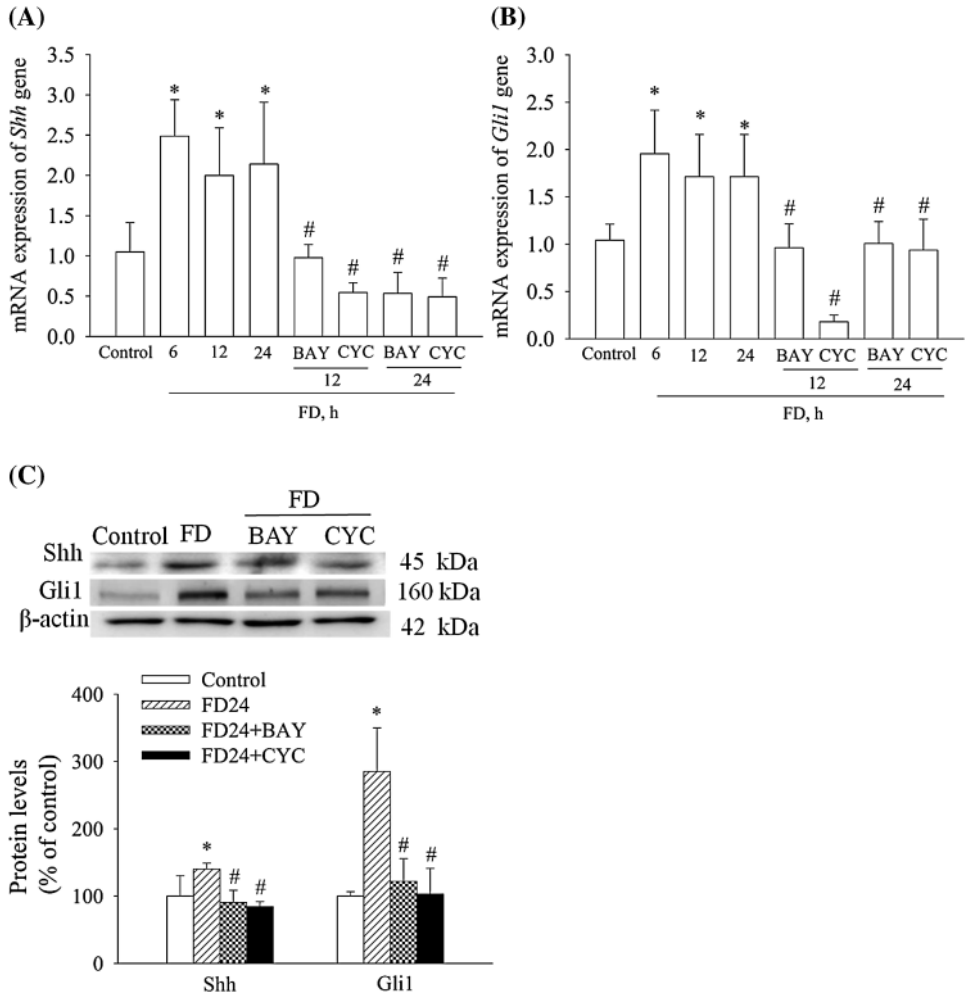

Fig. 6. Blockade effects of NF-κB pathway or Shh signaling on folate deficient (FD)-induced Shh induction and Shh–Gli signaling of HCT116 cells. HCT116 cells were cultivated in control or FD medium with or without 24 h pretreatment with cyclopamine (CYC: 10 μM) or Bay117082 (BAY: 3 μM). (**A** and **B**) Levels of (A) *Shh* and (B) *Gli1* transcripts by RT–PCR. (**C**) Production of Shh ligand and Gli1 transcription activator proteins by western blot analysis. Changes in PCR products were corrected for the corresponding level of *GUS* gene in the sample. Proteins were normalized by actin. Data are percentages of the control. Values are means ± standard deviations of three independent experiments. *Compared with the control; #compared with the FD group at the respective time point by Student's *t*-test at $P < 0.05$.

and that FD modified phosphorylation of the NF-κB complex (46), our data support the possibility that FD-associated posttranslational modifications and epigenetic regulation may modify NF-κB p65 binding to the *Shh* promoter region. As characterized in pancreatic cells, there are several putative binding sites for the nuclear NF-κB complex in the CpG island-rich region of the *Shh* promoter (24; Figure 3). Whether FD-disturbed one-carbon metabolism can elicit nuclear modification of the NF-κB complex or FD-induced epigenetic hypomethylation may modulate DNA binding of NF-κB p65 at all putative binding sites of the *Shh* promoter required studies.

One of the major findings in the present study is to demonstrate that FD-promoted the Shh signaling and NF-κB activation were under reciprocal regulation. Treatment of HCT116 cells with NF-κB pathway inhibitor abrogated FD-induced overproduction of Shh protein and Gli1 transcription activator, which was due, in part or in full, to the abovementioned transcriptional upregulation. Instead of affecting nuclear translocation and DNA-binding activity of nuclear NF-κB subunit p65, CYC treatment abolished FD-induced IκBα degradation and increased production of NF-κB p65 subunit and subsequently abrogated NF-κB pathway activation, as measured by suppression of the NF-κB target gene *TNFα*. The data suggest that regulation of NF-κB activation by Shh signaling could be compartmentalized in the cytosol, at least, at the IκBα degradation and subject to the FD-associated multistep regulatory process. Although the mechanisms by which FD promotes a positive signaling feedback loop of Shh and NF-κB signaling are not known, it has recently been proposed that Shh signaling acts on multiple upstream regulatory signals of the NF-κB pathway such as the Akt/Erk1/2 pathway in pancreatic tumorigenesis (49) and the RAS/Akt pathway in human melanomas (50). In renal cell carcinoma, both CYC treatment and Smo–Gli1 silencing inhibited the Akt/PI3K pathway as well as NF-κB activation (26). Cross interaction among the PI3K, mitogen-activated protein kinase and Shh pathways in esophageal cancer has been reported (51). Mitogen-activated protein kinase and Akt signaling in cancer cells may regulate the nuclear localization and transcriptional activity of Gli1. Such Akt activation in cultured fibroblasts can potentiate Gli activation by low-level Shh signaling to reinforce the activation of multiple target pathways (52). If that is the case in FD-colon cancer cells, it explains why CYC inhibited FD-induced *Gli1* expression at 12 h, but the expression partially recovered even with continuous CYC treatment for 24 h. Given that PI3K/Akt blocker (LY) abrogated the FD-induced NF-κB activation measured by IκBα degradation, the possibility of inducing a positive feedback loop in the PI3K/Akt–NF-κB–Shh pathway to mediate FD-enhanced invasion by colon cancer cells is highly likely. Analysis of the activation status of each signaling pathway in Smo–Gli–NF-κB or PI3K–Akt-silencing

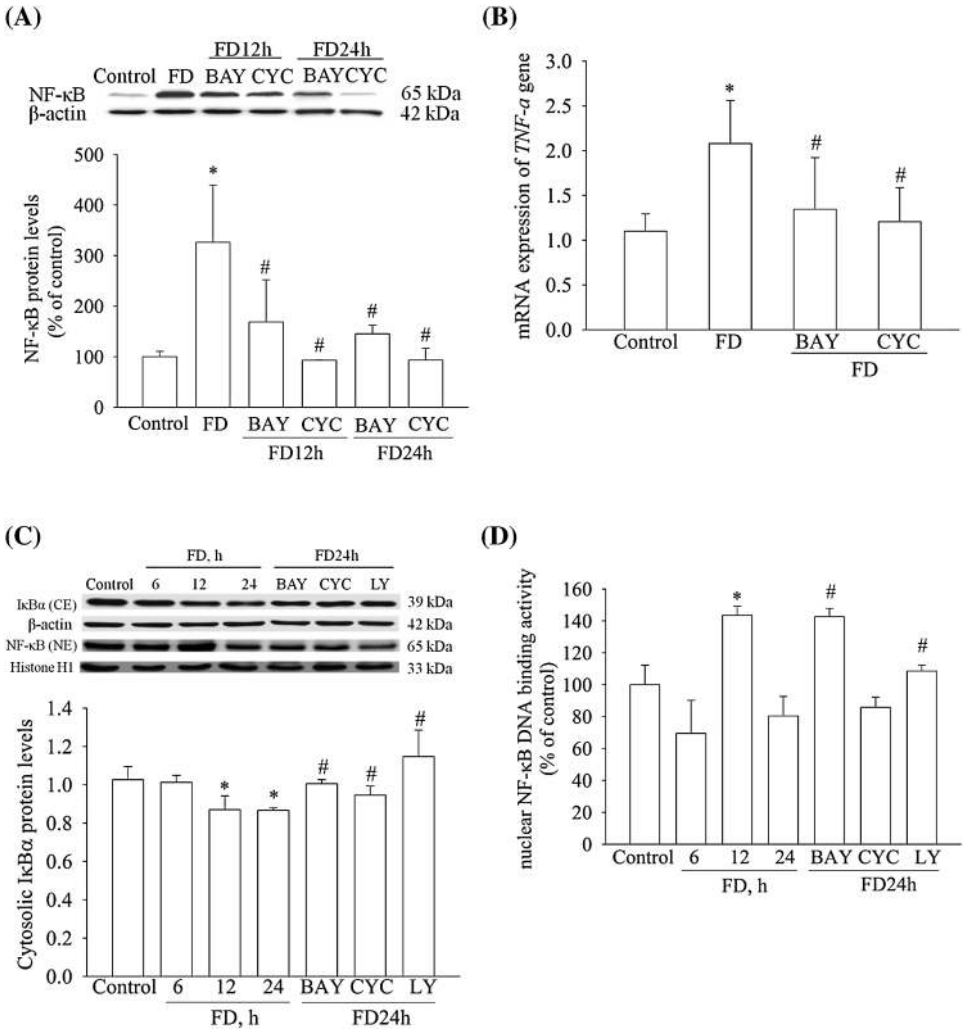

Fig. 7. Effects of blockade of NF-κB pathway or of Shh signaling on folate deficient (FD)-induced activation of NF-κB pathway in HCT116 cells. HCT116 cells were cultivated in control or FD medium with or without 24 h pretreatment with cyclopamine (CYC: 10 μM), Bay117082 (BAY: 3 μM) or LY294002 (LY: 20 μM). (**A**) Western blot analysis of NF-κB subunit p65 protein. (**B**) Transcript levels of *TNFα* as target gene of NF-κB pathway activation. (**C** and **D**) Effects of inhibitor treatments on FD-induced NF-κB pathway activation as measured by (C) IκBα degradation and nuclear translocation of NF-κB subunit p65 and (D) NF-κB DNA-binding activity. Proteins of cytosolic extracts (CE) were normalized against actin. Proteins of nuclear extracts (NE) were normalized against histone 1. NF-κB activation DNA binding was assayed by enzyme-linked immunosorbent. Values are means ± standard deviations of three independent experiments. *Compared with the control; #compared with the FD group at the respective time point by Student's *t*-test at $P < 0.05$.

FD-cells should provide additional insights into the reciprocal regulatory mechanisms and the sequential cross actions of these pathways.

In summary, our data identify folate deprivation as the metabolic stressor that enhances EMT and invasiveness of epithelial-adenocarcinoma-derived colon cancer cells. Through *Shh* promoter hypomethylation and cross-activation of the NF-κB pathway, FD activated Shh induction and Shh–Gli signaling to mediate invasion by colon cancer cells. FD may promote a positive feedback loop in the NF-κB–Shh pathway to reinforce multiple targets of EMT-associated signaling. These mechanisms are subjects for future studies. Clarification of the signal pathways involved as key biomarkers of FD-enhanced colonic cancer aggressiveness is of clinical significance in identifying therapeutic targets of better prognosis for colon cancer patients suffering from folate deficiency due to dietary insufficiency, metabolic stress or clinical etiology such as inflammatory bowel disease.

Supplementary material

Supplementary Table 1 and Figures 1 and 2 can be found at http://carcin.oxfordjournals.org/.

Funding

This study was funded by a 3-year grant from the National Science Council, Taiwan, Republic of China (NSC100-2320-B-030-005-MY3).

Acknowledgements

The authors acknowledge Dr Pao-Tien Chuang at University of California, San Francisco (UCSF) for his inspiration and advice on the Hh signaling project and on manuscript preparation.

Conflict of Interest Statement: None declared.

References

1. Jemal,A. *et al*. (2009) Cancer statistics. *CA Cancer J. Clin.*, **59**, 225–249.
2. Tol,J. *et al*. (2009) Chemotherapy, bevacizumab, and cetuximab in metastatic colorectal cancer. *N. Engl. J. Med.*, **360**, 563–572.
3. Hanahan,D. *et al*. (2000) The hallmarks of cancer. *Cell*, **100**, 57–70.
4. Huber,M.A. *et al*. (2005) Molecular requirements for epithelial–mesenchymal transition during tumor progression. *Curr. Opin. Cell Biol.*, **17**, 548–558.

5. Karhadkar,S.S. *et al*. (2004) Hedgehog signalling in prostate regeneration, neoplasia and metastasis. *Nature*, **431**, 707–712.
6. Feldmann,G. *et al*. (2007) Blockade of hedgehog signaling inhibits pancreatic cancer invasion and metastases: a new paradigm for combination therapy in solid cancers. *Cancer Res.*, **67**, 2187–2196.
7. Young,A.Y. *et al*. (2008) Sonic hedgehog signaling promotes motility and invasiveness of gastric cancer cells through TGF-β-mediated activation of the ALK5–Smad 3 pathway. *Carcinogenesis*, **29**, 480–490.
8. Liao,X. *et al*. (2009) Aberrant activation of hedgehog signaling pathway in ovarian cancers: effect on prognosis, cell invasion and differentiation. *Carcinogenesis*, **30**, 131–140.
9. Denef,N. *et al*. (2000) Hedgehog induces opposite changes in turnover and subcellular localization of patched and smoothened. *Cell*, **102**, 521–531.
10. Taipale,J. *et al*. (2002) Patched acts catalytically to suppress the activity of smoothened. *Nature*, **418**, 892–897.
11. Li,X. *et al*. (2006) Snail induction is an early response to Gli1 that determines the efficiency of epithelial transformation. *Oncogene*, **25**, 609–621.
12. Nagai,S. *et al*. (2008) Gli1 contributes to the invasiveness of pancreatic cancer through matrix metalloproteinase-9 activation. *Cancer Sci.*, **99**, 1377–1384.
13. Varnat,F. *et al*. (2009) Human colon cancer epithelial cells harbour active HEDGEHOG–GLI signalling that is essential for tumour growth, recurrence, metastasis and stem cell survival and expansion. *EMBO Mol. Med.*, **1**, 338–351.
14. Varnat,F. *et al*. (2010) Loss of WNT-TCF addiction and enhancement of HH-GLI1 signalling define the metastatic transition of human colon carcinomas. *EMBO Mol. Med.*, **2**, 1–18.
15. Varnat,F. *et al*. (2010) Hedgehog pathway activity is required for the lethality and intestinal phenotypes of mice with hyperactive Wnt signaling. *Mech. Dev.*, **127**, 73–81.
16. Nakashima,H. *et al*. (2006) Nuclear factor-κB contributes to hedgehog signaling pathway activation through sonic hedgehog induction in pancreatic cancer. *Cancer Res.*, **66**, 7041–7049.
17. Huber,M.A. *et al*. (2004) NF-κB is essential for epithelial–mesenchymal transition and metastasis in a model of breast cancer progression. *J. Clin. Invest.*, **114**, 569–581.
18. Aggarwal,B.B. (2004) Nuclear factor-κB: the enemy within. *Cancer Cell*, **6**, 203–208.
19. Aggarwal,B.B. *et al*. (2009) Targeting inflammatory pathways for prevention and therapy of cancer: short-term friend, long-term foe. *Clin. Cancer Res.*, **15**, 425–430.
20. Gupta,S.C. *et al*. (2011) Role of nuclear factor-κB-mediated inflammatory pathways in cancer-related symptoms and their regulation by nutritional agents. *Exp. Biol. Med. (Maywood)*, **236**, 658–671.
21. Wang,J.H. (2003) Endotoxin/lipopolysaccharide activates NF-{kappa}B and enhances tumor cell adhesion and invasion through a {beta}1 integrin-dependent mechanism. *J. Immunol.*, **170**, 795–804.
22. Ghosh,S. *et al*. (2002) Missing pieces in the NF-κB puzzle. *Cell*, **109**, S81–S96.
23. Hayden,M.S. *et al*. (2004) Signaling to NF-kappaB. *Genes Dev.*, **18**, 2195–2224.
24. Kasperczyk,H. *et al*. (2009) Characterization of sonic hedgehog as a novel NF-kappaB target gene that promotes NF-kappaB-mediated apoptosis resistance and tumor growth *in vivo*. *FASEB J.*, **23**, 21–33.
25. Yamasaki,A. *et al*. (2010) Nuclear factor kappaB-activated monocytes contribute to pancreatic cancer progression through the production of Shh. *Cancer Immunol. Immunother.*, **59**, 675–686.
26. Dormoy,V. *et al*. (2009) The sonic hedgehog signaling pathway is reactivated in human renal cell carcinoma and plays orchestral role in tumor growth. *Mol. Cancer*, **8**, 123–139.
27. Giovannucci,E. (2002) Epidemiologic studies of folate and colorectal neoplasia: a review. *J. Nutr.*, **132**, 2350S–2355S.
28. La Vecchia,C. *et al*. (2002) Dietary folate and colorectal cancer. *Int. J. Cancer*, **102**, 545–547.
29. Martinez,M.E. *et al*. (2004) Folate and colorectal neoplasia: relation between plasma and dietary markers of folate and adenoma formation. *Am. J. Clin. Nutr.*, **79**, 691–697.
30. Phelip,J.M. *et al*. (2008) Association of hyperhomocysteinemia and folate deficiency with colon tumors in patients with inflammatory bowel disease. *Inflamm. Bowel Dis.*, **14**, 242–248.
31. Choi,S.W. *et al*. (2002) Folate status: effects on pathways of colorectal carcinogenesis. *J. Nutr.*, **132**, 2413S–2418S.
32. Kim,Y. (2004) Folate and DNA methylation: a mechanistic link between folate deficiency and colorectal cancer? *Cancer Epidemiol. Biomarkers Prev.*, **13**, 511–519.
33. Shahi,M.H. *et al*. (2011) Expression and epigenetic modulation of sonic hedgehog–GLI1 pathway genes in neuroblastoma cell lines and tumors. *Tumor Biol.*, **32**, 113–127.
34. Fu,X. *et al*. (2010) Distinct expression patterns of hedgehog ligands between cultured and primary colorectal cancers are associated with aberrant methylation of their promoters. *Mol. Cell Biochem.*, **337**, 185–192.
35. Wang,L.H. *et al*. (2006) Increased expression of sonic hedgehog and altered methylation of its promoter region in gastric cancer and its related lesions. *Modern Pathol.*, **19**, 675–683.
36. Novakovic,P. *et al*. (2006) Effects of folate deficiency on gene expression in the apoptosis and cancer pathways in colon cancer cells. *Carcinogenesis*, **27**, 916–924.
37. Horne,D.W. *et al*. (1988) *Lactobacillus casei* microbiological assay of folic acid derivatives in 96-well microtiter plates. *Clin. Chem.*, **34**, 2357–2359.
38. Kitazawa,S. *et al*. (1998) Promoter structure of human sonic hedgehog gene. *Biochim. Biophys. Acta*, **1443**, 358–363.
39. Jeanes,A. *et al*. (2008) Cadherins and cancer: how does cadherin dysfunction promote tumor progression? *Oncogene*, **27**, 6920–6929.
40. Varner,J.A. *et al*. (1996) Integrins and cancer. *Cur. Opin. Cell Biol.*, **8**, 724.
41. Chatel,G. *et al*. (2007) Hedgehog signaling pathway is inactive in colorectal cancer cell lines. *Int. J. Cancer*, **121**, 2622–2627.
42. Berman,D.M. *et al*. (2003) Widespread requirement for Hedgehog ligand stimulation in growth of digestive tract tumours. *Nature*, **425**, 846–851.
43. Watkins,D.N. *et al*. (2003) Hedgehog signalling within airway epithelial progenitors and in small-cell lung cancer. *Nature*, **422**, 313–317.
44. Silver,A. *et al*. (2012) A distinct DNA methylation profile associated with microsatellite and chromosomal stable sporadic colorectal cancers. *Int. J. Cancer*, **130**, 1082–1092.
45. Lin,J.Y. (2011) *Folate Deficiency Promotes Invasion of Colon Adenocarcinoma Cells Through Epigenetic Regulation on Aberrant Activation of Hedgehog Signaling Pathway.* MS thesis, Department of Nutritional Science, Fu Jen University, Taiwan, Republic of China.
46. Chern,C.L. *et al*. (2001) Folate deficiency-induced oxidative stress and apoptosis are mediated via homocysteine-dependent overproduction of hydrogen peroxide and enhanced activation of NF-kappaB in human Hep G2 cells. *Biomed. Pharmacother.*, **55**, 434–442.
47. Chen,L.F. *et al*. (2001) Duration of nuclear NF-κB action regulated by reversible acetylation. *Science* **293**, 1653–1657.
48. Chen,L.F. *et al*. (2004) Shaping the nuclear action of NF-κB. *Nat. Rev. Mol. Cell Biol.*, **5**, 392–401.
49. Morton,J.P. *et al*. (2007) Sonic hedgehog acts at multiple stages during pancreatic tumorigenesis. *Proc. Natl Acad. Sci. USA*, **104**, 5103–5108.
50. Stecca,B. *et al*. (2007) Melanomas require HEDGEHOG–GLI signaling regulated by interactions between GLI1 and the RAS-MEK/AKT pathways. *Proc. Natl Acad. Sci. USA*, **104**, 5895–5900.
51. Wei,L.Y. *et al*. (2011) Cross-signaling among phosphoinositide-3 kinase, mitogen activated protein kinase and sonic hedgehog pathways exists in esophageal cancer. *Int. J. Cancer*, **129**, 275–284.
52. Morton,J.P. *et al*. (2007) Shh signaling and pancreatic cancer implications for therapy? *Cell Cycle*, **6**, 1553–1557.

Received September 26, 2011; revised February 27, 2012; accepted March 14, 2012